

Black hole/quantum machine learning correspondence

Jae-Weon Lee^{1,*} and Zae Young Kim^{2,†}

¹*Department of Electrical and Electronic Engineering, Jungwon University,
85 Munmu-ro, Goesan-eup, Goesan-gun, Chungcheongbuk-do, 28024, Republic of Korea.*
²*Spinor Media Inc, Seoul, 07332, Republic of Korea*

We explore a potential connection between the black hole information paradox and the double descent phenomenon in quantum machine learning. Information retrieval from Hawking radiation can be viewed through the lens of quantum linear regression over black hole microstates, with the Page time corresponding to the interpolation threshold, beyond which test error decreases despite overparameterization. Using the Marchenko–Pastur law, we derive the variance in test error for the quantum linear regression problem and show that the transition across the Page time is associated with a change in the rank structure of subsystems. This observation suggests a conceptual parallel between black hole physics and machine learning that may provide new perspectives for both fields.

I. INTRODUCTION

The black hole (BH) information paradox [1] presents a profound conflict between quantum mechanics and general relativity. According to Hawking’s semiclassical arguments [2], information about matter falling into a black hole appears to be irretrievably lost after evaporation, violating the unitarity of quantum theory. This tension has fueled decades of debate about the quantum nature of spacetime. There is a broad consensus that the Page time [3, 4] of a black hole represents a critical transition point, similar to a phase transition, at which information begins to emerge from the Hawking radiation.

Interestingly, a parallel conceptual structure has emerged in classical machine learning (CML) and quantum machine learning (QML), particularly in the so-called double descent phenomenon [5–7]. In traditional learning theory, increasing model complexity typically leads to overfitting and poor generalization. As the number of parameters P increases relative to the number of training samples N , the test error initially decreases due to reduced bias, then increases near the interpolation threshold where $P \approx N$ due to high variance, and finally decreases again in the overparameterized regime where $P \gg N$. This characteristic U-shaped behavior, followed by a second descent in test error, is known as the double descent phenomenon. The surprising recovery of generalization performance is now understood to be deeply tied to the statistical properties of the model’s data representation, often described by the spectral distribution of Gram or covariance matrices, such as the Marchenko-Pastur (MP) law [8, 9].

In this work, we propose a novel correspondence between the black hole information paradox and the double descent behavior in QML systems. We interpret the process of information recovery from Hawking radiation as analogous to linear regression over quantum states, where early-time evaporation corresponds to underparameterization, and the Page time [3, 4] marks the interpolation threshold. Beyond the Page time, information is well recoverable despite the apparent overparameterization of the Hilbert space.

We also show that the spectral structure of reduced density matrices during black hole evaporation exhibits an inversion symmetry in the effective dimension ratio $\alpha = P/N$, analogous to that in the MP distribution. The test error variance diverges at the Page time and decreases on either side, revealing a susceptibility-like behavior. This provides a physically meaningful analogue to generalization capacity in QML.

This unexpected correspondence between black hole physics and quantum learning offers a new conceptual bridge between quantum gravity and statistical learning theory. It also suggests that the recovery of information after the Page time is not a paradoxical feature but rather an emergent property of high-dimensional geometry and spectral transitions.

In section II we briefly review the relation between the Page curve and the MP distribution. In section III we investigate the double descent phenomenon in black hole evaporation. In section IV we discuss the results.

*Electronic address: scikid@jwu.ac.kr

†Electronic address: josephray@spinormedia.com

II. THE PAGE CURVE AND THE MP DISTRIBUTION

Black holes with the horizon area A have universal thermodynamic entropy given by the Bekenstein-Hawking entropy $S = A/4G$, which can reflect the number of microstates $|\psi_i\rangle \in \mathcal{H}_b$ with fixed expectation values for macroscopic observables. We model the Hawking radiation at a given time as occupying an Ω -dimensional subspace of the reservoir Hilbert space \mathcal{H}_r , which is maximally entangled with the black hole microstates. In this case the pure total state can be written as

$$|\psi\rangle = \sum_{i=1}^{\Omega} \frac{1}{\sqrt{\Omega}} |\psi_i\rangle \otimes |i\rangle \quad (1)$$

where $|i\rangle$ is a state of the radiation. Then, the reduced density matrix of the radiation is

$$\rho_r = \sum_{i,j=1}^{\Omega} \frac{1}{\Omega} \langle \psi_i | \psi_j \rangle |i\rangle \langle j|. \quad (2)$$

The density of eigenvalues of ρ_r can be given by [10, 11]

$$f(\lambda) = \frac{\Omega e^S}{2\pi\lambda} \sqrt{\left(\lambda - (\Omega^{-\frac{1}{2}} - e^{-\frac{S}{2}})^2\right) \left((\Omega^{-\frac{1}{2}} + e^{-\frac{S}{2}})^2 - \lambda\right)} + \delta(\lambda)(\Omega - e^S) \theta(\Omega - e^S) \quad (3)$$

$$\equiv \Omega^2 \tilde{f}(\tilde{\lambda}) \quad (4)$$

where

$$\tilde{f}(\tilde{\lambda}) = \frac{1}{2\pi\alpha\tilde{\lambda}} \sqrt{(\tilde{\lambda} - \tilde{\lambda}_-)(\tilde{\lambda}_+ - \tilde{\lambda})} + \delta(\tilde{\lambda}) \left(1 - \frac{1}{\alpha}\right) \theta(\alpha - 1), \quad (5)$$

$\tilde{\lambda} = \Omega\lambda$, $\tilde{\lambda}_{\pm} = \left(1 \pm \sqrt{\Omega/e^S}\right)^2$, and the first term is defined for $\tilde{\lambda}_- \leq \tilde{\lambda} \leq \tilde{\lambda}_+$. We will focus on black holes with this spectrum in this work and use the notation

$$\alpha \equiv \frac{\Omega}{e^S}. \quad (6)$$

Similar distributions also arise in the Gram matrix $\langle \psi_i | \psi_j \rangle$ that encodes the overlaps between black hole microstates. The Gram matrix of a large family of black hole microstates has been computed for various black holes including asymptotically AdS or Minkowski spacetimes, with or without angular momentum, electric charge, and supersymmetry [12–16].

According to Page's work, the entanglement entropy between the black hole interior and Hawking radiation outside follows a Page curve, reaching a maximum at the Page time when $\Omega \simeq e^S$. One can obtain the Page curve by integrating over $f(\lambda)$ [16]. The entanglement entropy S_r of the radiation can be calculated as

$$S_r = - \int d\lambda f(\lambda) \lambda \log \lambda = S + \log \alpha - \frac{1}{2\pi\alpha} \int_{\tilde{\lambda}_-}^{\tilde{\lambda}_+} d\tilde{\lambda} \sqrt{(\tilde{\lambda} - \tilde{\lambda}_-)(\tilde{\lambda}_+ - \tilde{\lambda})} \log \tilde{\lambda}, \quad (7)$$

which leads to [11]

$$S_r = \begin{cases} S + \log \alpha - \frac{\alpha}{2} & (0 < \alpha \leq 1), \\ S - \frac{1}{2\alpha} & (1 \leq \alpha). \end{cases} \quad (8)$$

Note that S_r exhibits an inversion symmetry with respect to $\alpha \leftrightarrow 1/\alpha$, or equivalently $\Omega \leftrightarrow e^S$. This calculation is consistent with Page's well-known result [4];

$$S_r = \log m - \frac{m}{2n}, \quad (9)$$

with $n \equiv \max\{\Omega, e^S\}$ and $m \equiv \min\{\Omega, e^S\}$ for $n, m \gg 1$. If $\Omega = e^S$, the entanglement entropy is $S_r = S - \frac{1}{2} \simeq S$.

Interestingly, the spectral density $\tilde{f}(\tilde{\lambda})$ coincides with the MP distribution in the random matrix theory:

$$f_{MP}(\tilde{\lambda}) \equiv \frac{1}{2\pi\alpha\tilde{\lambda}} \sqrt{(\tilde{\lambda} - \tilde{\lambda}_-)(\tilde{\lambda}_+ - \tilde{\lambda})} \theta(\tilde{\lambda} - \tilde{\lambda}_-) \theta(\tilde{\lambda}_+ - \tilde{\lambda}) + \delta(\tilde{\lambda}) \left(1 - \frac{1}{\alpha}\right) \theta(\alpha - 1), \quad (10)$$

which describes the asymptotic eigenvalue distribution of a large $N \times P$ random matrix X with $\alpha = P/N$, often arising in the following context. Let X be a random matrix with independent, identically distributed (i.i.d.) entries with zero mean and unit variance. If we define the covariance matrix as $\mathbf{C} = \frac{1}{N} X^\top X$ in the limit where both $N, P \rightarrow \infty$ with a fixed ratio α , the empirical eigenvalue distribution of \mathbf{C} converges almost surely to the MP distribution [8]. This distribution also provides insight into the double descent phenomenon in CML [17] (See Appendix A), and the formalism can be naturally extended to QML. By identifying $P = \Omega$ and $N = e^S$, one can draw a correspondence between QML and the BH physics, as elaborated in the following section.

III. DOUBLE DESCENT IN BLACK HOLE EVAPORATION

In this section, we investigate the manifestation of the double descent phenomenon in the context of black hole evaporation. Although QML shows promise for outperforming CML, it still lacks the practical impact and large-scale success that CML has already achieved. Recent studies have proposed that QML also exhibits the double descent phenomenon [18, 19], suggesting that QML models may benefit from having a large number of parameters.

In the quantum linear regression system, the model function F^β is defined as the quantum expectation value of an observable \mathcal{W} with respect to a quantum state ρ^β encoding information β :

$$F^\beta = \text{Tr}\{\rho^\beta \mathcal{W}\}, \quad (11)$$

where \mathcal{W} is a Hermitian operator on the P -dimensional Hilbert space. Measurement of \mathcal{W} on the state ρ^β yields an outcome whose expected value corresponds to F^β . We seek an operator \mathcal{W} that produces predictions close to the target values as in the classical linear regression described in Appendix A. In quantum feature space, the training data consists of quantum density matrices and labels:

$$\{(\rho^\beta, y^\beta)\}_{\beta=1}^N, \quad (12)$$

where $\rho^\beta \in \mathbb{C}^{P \times P}$ is a quantum density matrix and $y^\beta \in \mathbb{R}$ is a label.

In Ref. [20], it is shown that the dependence of the total state on the initial state becomes confined to the ancilla Hilbert space within the black hole. Consequently, the internal states $|\psi_i\rangle$ exhibit a degeneracy that cannot be detected through entanglement with the radiation. We will denote this degeneracy by an index $\beta = 1, \dots, N$, where the total number of degenerate states is expected to be $N = e^S$, and now the microstates $|\psi_i^\beta\rangle$ also have the index β . Therefore, we study the learning process based on the degenerate internal states encoded in the radiation.

In our framework, ρ^β corresponds to the reduced density matrix of the radiation $\rho_r^\beta \equiv \sum_{i,j=1}^P \frac{1}{P} \langle \psi_i^\beta | \psi_j^\beta \rangle |i\rangle\langle j|$ in Eq. (2) at a given time, and y^β represents a physical observable that can be extracted from ρ_r^β . We restrict our attention to diagonal \mathcal{W} . Then,

$$F^\beta = \sum_i^P \frac{1}{P} \langle \psi_i^\beta | \psi_i^\beta \rangle \mathcal{W}_{ii}. \quad (13)$$

Since ρ_r^β is related to the microstate $|\psi_i^\beta\rangle$ of BH, the regression can be interpreted as a form of information recovery. The observable \mathcal{W} is trained to map quantum radiation states ρ_r^β to these indices via linear measurements, such that $\text{Tr}\{\rho^\beta \mathcal{W}\} \approx y^\beta$. The learning process then corresponds to finding the optimal observable \mathcal{W} that best reconstructs the hidden internal index β solely from the radiation, thereby modeling information retrieval from Hawking radiation as a supervised learning problem. For the theoretical analysis that follows, we assume a hypothetical observer equipped with a complete theory of quantum gravity and knowledge of the true operator \mathcal{W} . The exact value of \mathcal{W} is not required for the purposes of our computation.

To closely follow the logic of classical linear regression shown in Appendix A, we define the data matrix $D \in \mathbb{C}^{N \times P}$ and the label vector $Y \in \mathbb{R}^N$ as:

$$D = \frac{1}{P} \begin{pmatrix} \langle \psi_1^1 | \psi_1^1 \rangle, \dots, \langle \psi_P^1 | \psi_P^1 \rangle \\ \vdots \\ \langle \psi_1^N | \psi_1^N \rangle, \dots, \langle \psi_P^N | \psi_P^N \rangle \end{pmatrix}, \quad Y = \begin{pmatrix} y^1 \\ \vdots \\ y^N \end{pmatrix}. \quad (14)$$

We also define a vectorized version of the operator \mathcal{W} as $\vec{\mathcal{W}} = (\mathcal{W}_{11}, \dots, \mathcal{W}_{PP})^\dagger$. Using these, one can follow a procedure similar to that of classical linear regression in Appendix. In our formalism, the number of parameters is given by $P = \Omega$. For the underparameterized regime ($P < N$), an optimal observable $\vec{\mathcal{W}}$ is obtained by solving a linear least squares problem:

$$\vec{\mathcal{W}}_{\text{under}} = \arg \min_{\vec{\mathcal{W}}} \|D\vec{\mathcal{W}} - Y\|^2, \quad (15)$$

which has a solution $\vec{\mathcal{W}}_{\text{under}} = (D^\dagger D)^{-1} D^\dagger Y$. In the overparameterized regime ($P > N$), the minimum-norm solution is $\vec{\mathcal{W}}_{\text{over}} = D^\dagger (DD^\dagger)^{-1} Y$ [18].

We consider a test quantum state ρ^t defined on the radiation Hilbert space \mathcal{H}_r . This can correspond to a test radiation state with a label value y^t . The prediction error for a test point (ρ^t, y^t) can be analyzed through the residual vector defined as $\epsilon \equiv Y - D\vec{\mathcal{W}}^*$, where \mathcal{W}^* is for the hypothetical optimal linear model. In the underparameterized regime, the prediction error becomes $\text{vec}(\rho^t)^\dagger (D^\dagger D)^{-1} D^\dagger \epsilon$, whereas in the overparameterized regime, it is given by $\text{vec}(\rho^t)^\dagger D^\dagger (DD^\dagger)^{-1} \epsilon + \text{vec}(\rho^t)^\dagger (D^\dagger (DD^\dagger)^{-1} D - I) \vec{\mathcal{W}}^*$. Here, the vectorized test state is $\text{vec}(\rho^t)^\dagger \equiv (\langle \psi_1^t | \psi_1^t \rangle, \dots, \langle \psi_P^t | \psi_P^t \rangle) / P$.

We focus on the first term (the variance) and derive it for each case, since the variance is essential for the double descent. For a given ρ^t the variance is usually proportional to $\|\vec{\mathcal{W}}^* - \vec{\mathcal{W}}_{\text{under}}\|^2$ for the underparameterized case. If Gaussian noise is present in the measurements, where $\epsilon \sim N(0, \sigma^2 I_N)$, then the variance is proportional to

$$\begin{aligned} \|\vec{\mathcal{W}}^* - \vec{\mathcal{W}}_{\text{under}}\|^2 &= \left\| \vec{\mathcal{W}}^* - (D^\dagger D)^{-1} D^\dagger Y \right\|^2 \\ &= \left\| \vec{\mathcal{W}}^* - (D^\dagger D)^{-1} D^\dagger D \vec{\mathcal{W}}^* - (D^\dagger D)^{-1} D^\dagger \epsilon \right\|^2 \\ &= \|(D^\dagger D)^{-1} D^\dagger \epsilon\|^2. \end{aligned} \quad (16)$$

Therefore, the average variance V over ϵ (up to a variance of ρ^t itself) is

$$\begin{aligned} V \equiv E_\epsilon \left[\|\vec{\mathcal{W}}^* - \vec{\mathcal{W}}_{\text{under}}\|^2 \right] &= E_\epsilon \left[\epsilon^\dagger D (D^\dagger D)^{-2} D^\dagger \epsilon \right] \\ &= \sigma^2 \text{Tr}(D (D^\dagger D)^{-2} D^\dagger) \\ &= \sigma^2 \text{Tr}((D^\dagger D)^{-1}). \end{aligned} \quad (17)$$

In the limit $P = \alpha N \rightarrow \infty$, the above error approaches $\sigma^2 \alpha S(0)$ [9] for D associated with ρ_r in Eq. 2, where

$$S(z) \equiv \int \frac{1}{\lambda - z} f_{\text{MP}}(\lambda) d\lambda \quad (18)$$

is the Stieltjes transform. Using the resolvent method one can obtain $S(0) = 1/(1 - \alpha)$ and then

$$V = E_\epsilon \left[\|\vec{\mathcal{W}}^* - \vec{\mathcal{W}}_{\text{under}}\|^2 \right] = \sigma^2 \frac{\alpha}{1 - \alpha}, \quad (19)$$

which diverges at the interpolation threshold ($\alpha = 1$). Therefore, the test error diverges at the interpolation threshold (i.e., the Page time) and decreases with increasing α , exhibiting the double descent phenomenon in the quantum linear regression system and black holes. Using the inversion symmetry one can also obtain the variance for the overparametrized case [9]:

$$V = E_\epsilon \left[\|\vec{\mathcal{W}}^* - \vec{\mathcal{W}}_{\text{over}}\|^2 \right] = \frac{\sigma^2}{\alpha - 1}, \quad (20)$$

where $\alpha > 1$. Fig. 1 shows the Page curve and V as functions of α with $\sigma = 1$. One can see that BH evaporation can be interpreted as a double descent phenomenon in QML.

In deep learning, the inverse of the Hessian of the loss function characterizes the model's sensitivity to parameter perturbations and, in our case, is proportional to the variance $V \propto S(0)$. The presence of eigenvalues near zero leads to a divergence in the Stieltjes transform $S(0)$, resulting in a sharp increase in both the variance and the test error. The variance corresponds to quantum susceptibility at the interpolation threshold, where the sensitivity of information recovery changes abruptly, serving as an indicator of a quantum phase transition [21].

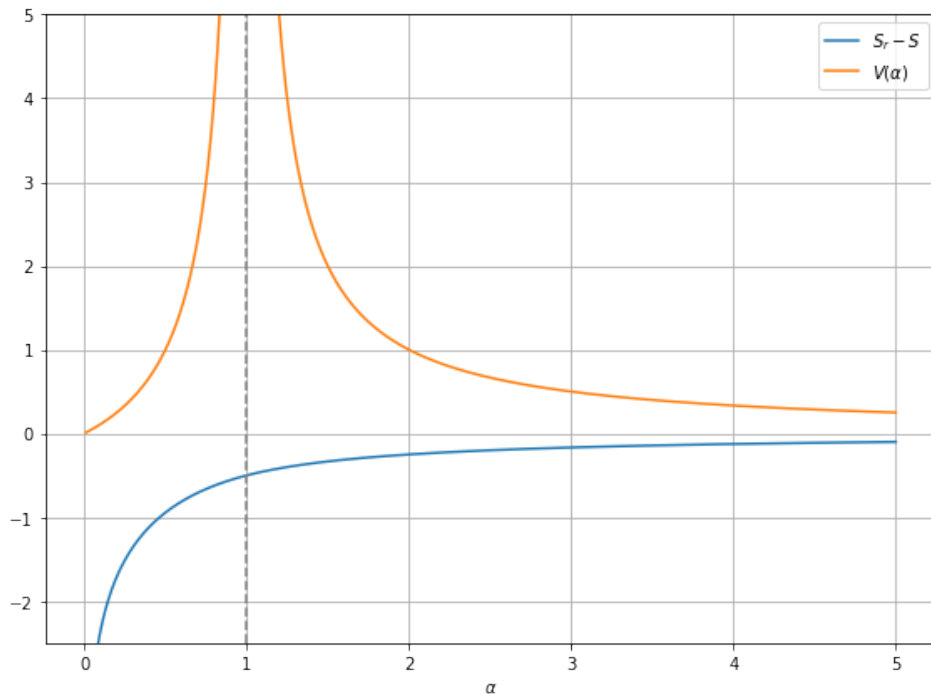


FIG. 1: The Page curve ($S_r - S$) and the variance V are plotted as functions of the ratio $\alpha = \Omega/e^S = P/N$. The variance exhibits a divergence at the Page time ($\alpha = 1$), signaling a quantum phase transition in the information retrieval process.

To understand the role of zero modes in the MP distribution let us define the projection operator $\Pi = D^\dagger (DD^\dagger)^{-1} D$, which projects any operator onto the subspace spanned by the rows of D . If the condition $\Pi \text{vec}(\rho^t) = \text{vec}(\rho^t)$ holds, then ρ^t lies entirely within the radiation subspace. In such a case, the test state ρ^t can be faithfully reconstructed from the radiation with the learned \mathcal{W} , and the expectation value y^t is exactly recoverable, in principle. This condition becomes feasible only after the Page time. Before the Page time, when $P < N$ (i.e., the number of radiation degrees of freedom is smaller than that of the black hole interior), the radiation subspace remains insufficient for full reconstruction. As a result, many test states ρ^t do not lie in the image of Π , and recovery fails. In contrast, after the Page time, when $P > N$, the radiation space becomes overcomplete. This confirms that the information contained in ρ^t is fully recoverable from the radiation subsystem alone only after the Page time or the interpolation threshold. Table 1 summarizes the correspondence between BH physics and QML.

| Concept | Black Hole physics | Quantum machine learning |
|---------------------------------|--|--|
| Dimension ratio (α) | Hilbert space ratio (radiation vs BH): $\alpha = \Omega/e^S$ | Parameters vs data samples ratio: $\alpha = P/N$ |
| Critical point ($\alpha = 1$) | Page time | Interpolation threshold |
| $\alpha < 1$ | ρ_r full-rank | Underparameterized regime |
| $\alpha > 1$ | ρ_r rank-deficient (appearance of zero modes) | Overparameterized regime |

TABLE I: Black hole/QML correspondence dictionary

This transition reflects a structural shift in how and where information is stored and accessed, revealing an inversion of informational roles between the black hole interior and the radiation. The $\alpha \leftrightarrow 1/\alpha$ duality suggests a deeper complementarity between observers: what is inaccessible to an external observer before the Page time becomes accessible afterward, and vice versa.

IV. DISCUSSION

The information recovery transition during black hole evaporation is captured spectrally through a rank transition in the reduced density matrices. Using the Marchenko–Pastur distribution, we model black hole evaporation as a

quantum linear regression process. This machine learning viewpoint reinforces the quantum gravitational insight that black hole information becomes distinguishable in Hawking radiation only after the Page time, which is encoded in the nontrivial spectral reshaping of ρ_r .

Our framework provides a novel approach for interpreting both black hole information recovery and quantum machine learning generalization as manifestations of information-induced geometry, where the inversion symmetry plays a role. The bias-variance structure in quantum machine learning corresponds structurally to the information dynamics of black hole evaporation. A black hole functions as a quantum information processing system, and its radiation structure exhibits deep analogies with statistical learning systems. It invites the use of machine learning diagnostics such as spectral analysis, resolvent methods, and capacity measures to probe quantum gravity, while suggesting that principles from black hole thermodynamics may shed light on the generalization behavior and representational structure of quantum machine learning models.

Appendix A: Double descent in CML and Marchenko-Pastur distribution

We review a classical linear regression problem which is a representative machine learning example that illustrates the double descent phenomenon. Consider a set of N training data [7]

$$\mathcal{D} \equiv \{(\vec{x}_n, y_n)\}_{n=1}^N \quad (\text{A1})$$

with covariates $\vec{x}_n \in \mathbb{R}^P$ and target values $y_n \in \mathbb{R}$. In linear regression problems, the aim is to find a linear function $F(\vec{x}) = \vec{x} \cdot \vec{w}$ with an ideal weight \vec{w} which accurately predicts a new target y for an input x based on the dataset \mathcal{D} . Our objective is to estimate linear parameters $\hat{\vec{w}} \in \mathbb{R}^P$ such that:

$$\vec{x} \cdot \hat{\vec{w}} \approx y. \quad (\text{A2})$$

In other words, we seek a weight vector $\hat{\vec{w}}$ that produces predictions close to the target values through a linear combination of input features. It is convenient to use a matrix notation to treat the features as row vectors of $X \in \mathbb{R}^{N \times P}$ and define

$$Y \equiv \begin{bmatrix} y_1 \\ \vdots \\ y_N \end{bmatrix} \in \mathbb{R}^{N \times 1} \quad (\text{A3})$$

In typical machine learning problems, the test error is often governed by two key factors: the number of model parameters P and the number of training samples N , especially in the regime where both P and N are very large.

For an underparameterized regime ($P < N$), we can solve the least-squares minimization problem [7]:

$$\hat{\vec{w}}_{\text{under}} \equiv \arg \min_{\vec{w}} \frac{1}{N} \sum_n \|\vec{x}_n \cdot \vec{w} - y_n\|^2 = \arg \min_{\vec{w}} \|X\vec{w} - Y\|^2, \quad (\text{A4})$$

which has a solution:

$$\hat{\vec{w}}_{\text{under}} = (X^T X)^{-1} X^T Y. \quad (\text{A5})$$

In the overparameterized regime ($P > N$), the optimization problem becomes ill-posed, as there are fewer constraints than parameters. In this case one can instead consider the following optimization problem:

$$\hat{\vec{w}}_{\text{over}} \equiv \arg \min_{\vec{w}} \|\vec{w}\|^2 \quad \text{s.t.} \quad \forall n \in \{1, \dots, N\}, \quad \vec{x}_n \cdot \vec{w} = y_n, \quad (\text{A6})$$

which has a solution with Gram matrix $XX^T \in \mathbb{R}^{N \times N}$:

$$\hat{\vec{w}}_{\text{over}} = X^T (XX^T)^{-1} Y. \quad (\text{A7})$$

If we have a Gaussian noise $\epsilon \sim N(0, \sigma^2 I_N)$ in measurements, then $Y = X\vec{w} + \epsilon$ and the variance in the underparameterized regime is proportional to

$$\begin{aligned} \|\vec{w} - \hat{\vec{w}}_{\text{under}}\|^2 &= \|\vec{w} - (X^T X)^{-1} X^T Y\|^2 \\ &= \|\vec{w} - (X^T X)^{-1} X^T X\vec{w} - (X^T X)^{-1} X^T \epsilon\|^2 \\ &= \|(X^T X)^{-1} X^T \epsilon\|^2, \end{aligned} \quad (\text{A8})$$

where \vec{w} is the ideal weight. The average error over ϵ becomes

$$\begin{aligned} E_\epsilon [\|\vec{w} - \hat{\vec{w}}_{\text{under}}\|^2] &= E_\epsilon [\epsilon^T X (X^T X)^{-2} X^T \epsilon] \\ &= \sigma^2 \text{Tr}(X (X^T X)^{-2} X^T) \\ &= \sigma^2 \text{Tr}((X^T X)^{-1}) \end{aligned} \quad (\text{A9})$$

In the limit $P = \alpha N \rightarrow \infty$, the above error approaches $\sigma^2 \alpha S(0)$ for a Gaussian random matrix X , where

$$S(z) = \int \frac{1}{\lambda - z} f_{\text{MP}}(\lambda) d\lambda \quad (\text{A10})$$

is the Stieltjes transform. Using the resolvent method one can obtain $S(0) = 1/(1 - \alpha)$ and

$$E_\epsilon \left[\|w - \hat{w}_{under}\|^2 \right] = \sigma^2 \frac{\alpha}{1 - \alpha}, \quad (\text{A11})$$

which diverges at the interpolation threshold ($\alpha = 1$). Therefore, the test error diverges at the interpolation threshold.

For the overparameterized case, the roles of P and N are exchanged, thus α is replaced by $\frac{1}{\alpha}$ and the variance term converges to $\sigma^2 \frac{\frac{1}{\alpha}}{1 - \frac{1}{\alpha}} = \sigma^2 \frac{1}{\alpha-1}$ for $P = \alpha N \rightarrow \infty$. Hence, the test error decreases once more as P increases when $P > N$.

[1] A. Almheiri, T. Hartman, J. Maldacena, E. Shaghoulian, and A. Tajdini, Rev. Mod. Phys. **93**, 035002 (2021), 2006.06872.

[2] S. W. Hawking, Phys. Rev. D **14**, 2460 (1976).

[3] D. N. Page, Phys. Rev. Lett. **71**, 1291 (1993).

[4] D. N. Page, Phys. Rev. Lett. **71**, 3743 (1993).

[5] M. Belkin, D. Hsu, S. Ma, and S. Mandal, Proc. Natl. Acad. Sci. USA **116**, 15849 (2019).

[6] M. Loog, T. Viering, A. Mey, J. H. Krijthe, and D. M. J. Tax, Proc. Natl. Acad. Sci. USA **117**, 10625 (2020).

[7] R. Schaeffer, M. Khona, Z. Robertson, A. Boopathy, K. Pistunova, J. W. Rocks, I. R. Fiete, and O. Koyejo (2023), 2303.14151.

[8] V. Marchenko and L. Pastur, Math. USSR Sbornik **1**, 457 (1967).

[9] R. Speicher and J. Hoffmann, *High-dimensional analysis: Random matrices and machine learning* (2023), lecture notes, Saarland University, Summer Term 2023.

[10] G. Penington, S. H. Shenker, D. Stanford, and Z. Yang, JHEP **03**, 205 (2022), 1911.11977.

[11] K. Kawabata, T. Nishioka, Y. Okuyama, and K. Watanabe, JHEP **05**, 062 (2021), 2102.02425.

[12] J. M. V. Balasubramanian, A. Lawrence and M. Sasieta, Phys. Rev. X **14**, 011024 (2024).

[13] J. M. M. V. Balasubramanian, A. Lawrence and M. Sasieta, Phys. Rev. Lett. **132**, 141501 (2024).

[14] J. M. M. M. S. A. Climent, R. Emparan and A. V. López, Phys. Rev. D **109**, 086024 (2024).

[15] W. Mück, Phys. Rev. D **109**, 126001 (2024), 2403.05241.

[16] N. Iizuka and M. Nishida, JHEP **12**, 212 (2025), 2410.04679.

[17] P. Mehta, M. Bukov, C. H. Wang, A. G. R. Day, C. Richardson, C. K. Fisher, and D. J. Schwab, Phys. Rep. **810**, 1 (2019).

[18] M. Kempkes, A. Ijaz, E. Gil-Fuster, C. Bravo-Prieto, J. Spiegelberg, E. van Nieuwenburg, and V. Dunjko (2025), 2501.10077.

[19] J. Tomasi, S. Anthoine, and H. Kadri (2025), 2503.17020.

[20] S. L. Braunstein and A. K. Pati, Phys. Rev. Lett. **98**, 080502 (2007), gr-qc/0603046.

[21] J. W. Rocks and P. Mehta, Physical Review Research **4**, 013201 (2022).